

Impact ionization rates for Si, GaAs, InAs, ZnS, and GaN in the *GW* approximation

Takao Kotani

Department of Applied Mathematics and Physics, Tottori University, Tottori 680-8552, Japan

Mark van Schilfgaarde

School of Materials, Arizona State University, Tempe, Arizona 85284, USA

(Received 3 December 2009; revised manuscript received 20 January 2010; published 4 March 2010)

We present first-principles calculations of the impact ionization rate (IIR) in the *GW* approximation (GWA) for semiconductors. The IIR is calculated from the quasiparticle (QP) width in the GWA, since it can be identified as the decay rate of a QP into lower energy QP plus an independent electron-hole pair. The quasiparticle self-consistent *GW* method was used to generate the noninteracting Hamiltonian the GWA requires as input. Small empirical corrections were added so as to reproduce experimental band gaps. Our results are in reasonable agreement with previous work, though we observe some discrepancy. In particular we find high IIR at low energy in the narrow gap semiconductor InAs.

DOI: [10.1103/PhysRevB.81.125201](https://doi.org/10.1103/PhysRevB.81.125201)

PACS number(s): 72.20.Jv, 71.15.Qe

I. INTRODUCTION

The electron-initiated impact ionization is a fundamental process in semiconductors where a high energy electron decays into another low-energy electron together with an electron-hole pair.¹ The impact ionization rate (IIR), which originates from the coulomb interaction between electrons, is a critical factor affecting transport under high-electric field, as described by the Boltzmann transport equation (BTE). It is important in narrow gap semiconductors, especially for ultrasmall devices. Impact ionization is also used in avalanche photodiodes, and to supply electron-hole pairs for electroluminescence. Recently it has stimulated interest as a mechanism to improve efficiency in photovoltaic devices.²

The IIR has been calculated with empirical pseudopotentials (EPPs) in order to include realistic energy bands.³⁻⁷ Sano and Yoshii calculated the IIR for Si (Refs. 4 and 5) and obtained reasonable agreement with experimental data. They also studied other materials,⁶ treating the transition matrix element M as a parameter (constant matrix approximation). Jung *et al.*⁷ used an EPP to calculate the IIR in GaAs. They calculated M including explicit calculation of the dielectric function $\epsilon(\mathbf{q}, \omega)$, rather than assuming a model form.

Recently, two groups have calculated the IIR using the density-functional formalism to generate the one-body eigenfunctions and energy bands. Because the standard local density approximation (LDA) underestimates semiconductor bandgaps while the IIR is very sensitive to this quantity, the standard LDA is not suitable. Picozzi *et al.* used a screened-exchange generalization⁸ of the LDA,^{9,10} and Kuligk *et al.* employed the exact exchange^{11,12} formalism.¹³ Both groups used model dielectric functions for the dynamically screened coulomb interaction $W(\mathbf{r}, \mathbf{r}', \omega)$.

Here, we will present (nearly) *ab initio* calculations of the IIR without model assumptions. First, our noninteracting Hamiltonian H^0 is generated within quasiparticle (QP) self-consistent *GW* (QSGW) formalism. We have shown that QSGW works very well for wide range of materials.¹⁴⁻¹⁸ Because the IIR is highly sensitive to the band gaps, we add a small empirical scaling of the exchange-correlation potential so as to reproduce the experimental fundamental gap E_G .

Corrections for semiconductors are small and systematic as shown below. Second, W is calculated from the QSGW noninteracting Hamiltonian. The IIR is identified with the decay rate (or linewidth) of the QP, which is calculated from the imaginary part of the self-energy, as we describe below. Our method, thus, contains only one parameter, to correct the band gap. As we have shown,¹⁹ this parameter is small and is approximately independent of material. In principle our method can predict the IIR in unknown systems, and also for inhomogeneous systems such as grain boundaries, quantum dots, or impurities, where the IIR should be strongly enhanced because momentum conservation is much more easily satisfied. Thus, the present *ab initio* method should be superior to prior approaches. Applications to such systems will be useful in devices that need to suppress or enhance electron-hole pair-generation from impact ionization.

After a theoretical discussion, we present some results. They are in reasonable agreement with previous calculations, except for InAs where IIR is calculated to be much higher than what Sano and Yoshii found.⁶

II. METHOD

The first step is to determine a good one-body Hamiltonian H^0 , which describes QPs. We obtain H^0 from QSGW calculations.¹⁴⁻¹⁶ As we explain in Sec. III, we follow Ref. 19, and modify H^0 by a simple empirical scaling (α correction) to ensure the fundamental gap reproduces experiment. From this modified H^0 , we obtain a set of eigenvalues $\{\epsilon_{\mathbf{k}n}\}$ and eigenfunctions $\{\Psi_{\mathbf{k}n}\}$, which are used to calculate the self-energy $\Sigma(\mathbf{r}, \mathbf{r}', \omega)$ within the *GW* approximation (GWA), $\Sigma = iG \times W$. The inverse of the QP lifetime $\tau_{\mathbf{k}n}^{-1}$ is obtained from the imaginary part of Σ as

$$\tau_{\mathbf{k}n}^{-1} = \frac{2Z_{\mathbf{k}n}}{\hbar} |\text{Im} \Sigma_{\mathbf{k}n}|, \quad (1)$$

where $\text{Im} \Sigma_{\mathbf{k}n} = \langle \Psi_{\mathbf{k}n} | \text{Im} \Sigma(\epsilon_{\mathbf{k}n}) | \Psi_{\mathbf{k}n} \rangle = \int d^3r \int d^3r' \Psi_{\mathbf{k}n}^*(\mathbf{r}) \times \text{Im} \Sigma(\mathbf{r}, \mathbf{r}', \epsilon_{\mathbf{k}n}) \Psi_{\mathbf{k}n}(\mathbf{r}')$. By $\text{Im} \Sigma(\epsilon_{\mathbf{k}n})$ we mean the anti-Hermitian part. $Z_{\mathbf{k}n}$ is the wave function renormalization fac-

tor to represent the QP weight. \mathbf{k} denotes the wave vector in the first Brillouin zone (BZ), and n the band index. The expression Eq. (1) for $\tau_{\mathbf{k}n}^{-1}$ is derived in Appendix B of Ref. 20. $\text{Im } \Sigma$ is obtained from the imaginary part of the convolution of G and W . For an unoccupied state $\mathbf{k}n$, it is

$$\text{Im } \Sigma_{\mathbf{k}n} = - \int d^3r d^3r' \sum_{\mathbf{k}'n'} \Psi_{\mathbf{k}n}^*(\mathbf{r}) \Psi_{\mathbf{k}'n'}(\mathbf{r}) \Psi_{\mathbf{k}'n'}^*(\mathbf{r}') \Psi_{\mathbf{k}n}(\mathbf{r}') \times \pi \text{Im } W(\mathbf{r}, \mathbf{r}', \varepsilon_{\mathbf{k}n} - \varepsilon_{\mathbf{k}'n'}), \quad (2)$$

where states $\mathbf{k}'n'$ are restricted to those for which $\varepsilon_{\mathbf{F}} < \varepsilon_{\mathbf{k}'n'} < \varepsilon_{\mathbf{k}n}$. W is calculated in the random phase approximation (RPA) as

$$W = v + v\chi v = (1 - v\chi_0)^{-1}v, \quad (3)$$

where v is the coulomb interaction; χ is the full polarization function in the RPA, and χ_0 is the non-interacting polarization function. With Eqs. (1)–(3), $\tau_{\mathbf{k}n}^{-1}$ is calculated from H^0 in principle. In the Lehmann representation, χ is

$$\chi(\mathbf{r}, \mathbf{r}', \omega) = \sum_m \langle 0 | \hat{n}(\mathbf{r}) | m \rangle \langle m | \hat{n}(\mathbf{r}') | 0 \rangle \times \left(\frac{1}{\omega - \omega_m - i\delta} - \frac{1}{\omega + \omega_m + i\delta} \right), \quad (4)$$

where $|m\rangle$ denotes the eigenstates (intermediate states) with excitation energy ω_m relative to the ground state $|0\rangle$. Here, $\hat{n}(\mathbf{r})$ is the density operator.

In the RPA, $|m\rangle$ are the eigenfunctions of a two-body (one electron and one hole) eigenvalue problem in the RPA. In simple cases such as the homogeneous electron gas, $|m\rangle$ for high ω_m are identified as plasmons; $|m\rangle$ for low ω_m are as independent motions of an electron and a hole. Thus, $\tau_{\mathbf{k}n}^{-1}$ for low-energy electrons calculated in GWA can be identified as the transition probability to such states for the independent motion of an electron and a hole together with an electron; that is, we identify $\tau_{\mathbf{k}n}^{-1}$ as the IIR.

There are some questionable points for the identification. It might be not so easy in some cases to identify a state $|m\rangle$ as such a independent motion because the electron-hole pair can be hybridized with plasmons. However, such hybridization is sufficiently small for the simple semiconductors treated here, because plasmons appear only at high energies as $\omega_m \gtrsim 1$ Ry. Another problem is that the final state consisting of two electrons and one hole is not symmetrized for the electrons in the GWA. Thus Fermi statistics are not satisfied. Below we discuss how much error it causes.

Our formula [Eq. (1)] for $\tau_{\mathbf{k}n}^{-1}$ is different from the customary expression found in the literature,^{3–7} e.g., see Eq. (1) in Ref. 3. It is written as

$$\tau_{\mathbf{k}n}^{-1} = \frac{4\pi}{\hbar} \sum_{\mathbf{k}'n'} \sum_{\mathbf{k}_1n_1} \sum_{\mathbf{k}_2n_2} |M|^2 \times \delta(\varepsilon_{\mathbf{k}n} - \varepsilon_{\mathbf{k}'n'} - \varepsilon_{\mathbf{k}_1n_1} + \varepsilon_{\mathbf{k}_2n_2}), \quad (5)$$

where $|M|^2 = \frac{1}{2}(|M_D|^2 + |M_E|^2 + |M_D - M_E|^2)$ includes both direct and exchange processes. The sum over $\mathbf{k}', \mathbf{k}_1, \mathbf{k}_2$ is restricted to satisfy $\mathbf{k} = \mathbf{k}' + \mathbf{k}_1 - \mathbf{k}_2$. The matrix element M_D for the direct process is

$$M_D = \left| \int d^3r d^3r'' \Psi_{\mathbf{k}n}(\mathbf{r}) \Psi_{\mathbf{k}'n'}^*(\mathbf{r}) \times W(\mathbf{r}, \mathbf{r}'', \varepsilon_{\mathbf{k}n} - \varepsilon_{\mathbf{k}'n'}) \Psi_{\mathbf{k}_1n_1}^*(\mathbf{r}'') \Psi_{\mathbf{k}_2n_2}(\mathbf{r}'') \right|. \quad (6)$$

M_E for the exchange process is the same as M_D , except that the two electrons in final states ($\mathbf{k}'n' \leftrightarrow \mathbf{k}_1n_1$) are exchanged. Equation (5) can be derived in time-dependent perturbation theory, where the final states consists of two electrons and one hole. This is based on the physical picture that W causes transitions between the Fock states made of QPs. However, the final states made of the three QPs are interacting each other. Thus such a picture do not necessarily well defined. This is related to a fundamental problem about how to mimic the quantum theory by the BTE. Definition of the IIR suitable for the BTE is somehow ambiguous. The difference between Eqs. (1) and (5) is related to the ambiguity. One is not necessarily better than the other.

To compare Eq. (1) with Eq. (5), let us assume that $\text{Im } \chi_0$ is small enough. Then we have

$$\text{Im } W \approx W_R \text{Im } \chi_0 W_R, \quad (7)$$

from Eq. (3), where $W_R = (1 - v \text{Re } \chi_0)^{-1}v$. $\text{Re } \chi_0$ denotes the Hermitian (real) part of χ_0 . If we apply Eq. (7) to Eq. (2), Eq. (1) is reduced to an expression similar to Eq. (5),

$$\tau_{\mathbf{k}n}^{-1} \approx \frac{4\pi Z_{\mathbf{k}n}}{\hbar} \sum_{\mathbf{k}'n'} \sum_{\mathbf{k}_1n_1} \sum_{\mathbf{k}_2n_2} |M_D|^2 \times \delta(\varepsilon_{\mathbf{k}n} - \varepsilon_{\mathbf{k}'n'} - \varepsilon_{\mathbf{k}_1n_1} + \varepsilon_{\mathbf{k}_2n_2}), \quad (8)$$

where M_D is defined in Eq. (6) but with W_R instead of W . Through Eq. (8) we can elucidate the differences between Eqs. (1) and (5) as follows:

(a) Eq. (8) [and thus Eq. (1)] contain the Z factor. This is because Eq. (5) was derived without taking into account the modification of QPs by the coulomb interaction. Typically $Z_{\mathbf{k}n}$ is ~ 0.8 .

(b) Eqs. (1) and (8) do not include M_E contributions. In the extreme case when $M_E = \frac{1}{2}M_D$, $|M|^2 = 0.75 \times |M_D|^2$. This occurs in the Hubbard model when W is a point interaction; the Feynman diagrams for M_D and M_E become the same except for their sign. Theoretically, including M_E is advantageous because it symmetrizes the two electrons in the final state (though only for $\text{Im } \chi_0$ in the linear response regime). Fermi statistics are not perfectly satisfied because not all the exchange-pair diagrams are included. Omitting the exchange contribution reduces the IIR by a factor 0.75 at most, as explained above.

(c) Eq. (8) contains only the real part of W , in contrast to Eq. (5). The difference originates from higher order contributions to $\text{Im } \chi_0$. Moreover, when Eq. (7) is not satisfied there are further higher-order contributions to $\text{Im } \chi_0$.

We may have to pay attention to these differences. For small $\text{Im } \chi_0$, (a) and (b) predominate, and the difference between Eq. (1) and the Kane formula Eq. (5) should be a factor in the range 0.5 to 1. However, this difference is relatively minor on the log scale in the figure.

TABLE I. Eigenvalues of semiconductors relative to the valence band maximum at Γ . The QSGW column depict results without spin-orbit coupling; values in parentheses include spin-orbit coupling. Column QSGW α shows values after scaling defined in Eq. (9). α is chosen so that the QSGW α potential (without spin-orbit coupling) reproduces the experimental minimum band gap at room temperature. See Eq. (9) and its explanations.

Si	Expt. ^a	QSGW	QSGW α ($\alpha=0.85$)
Γ_{15c}	3.34	3.45(3.41)	3.32
L_{6c}	2.04	2.35	2.21
E_g	1.12	1.23(1.11)	1.12
$\Gamma_{2'c}$	4.15	4.38	4.21
GaAs			
Expt. ^a	QSGW	QSGW α ($\alpha=0.68$)	
Γ_{6c}	1.42	1.93(1.81)	1.42
L_{6c}	1.66	2.11	1.72
X_{6c}	1.97	2.12	1.90
Γ_{7c}	4.50	4.74	4.42
InAs			
EmpPP ^b	QSGW	QSGW α ($\alpha=0.65$)	
Γ_{6c}	0.37	0.79(0.68)	0.38
L_{6c}	1.53	1.86	1.51
X_{6c}	2.28	2.10	1.90
Γ_{7c}	4.39	4.84	4.51
ZnS			
Expt. ^a	QSGW	QSGW α ($\alpha=0.83$)	
Γ_{6c}	3.68	4.04(4.01)	3.68
L_{6c}		5.45	5.05
X_{6c}		5.05	4.74
Γ_{7c}		8.67	8.26

^aExperimental data at room temperature, taken from Ref. 21.

^bEmpirical pseudopotential data are taken from Ref. 21. The experimental direct gap is ~ 0.4 eV.

III. RESULTS

Here, we treat Si, GaAs, InAs, zincblende ZnS, and wurtzite GaN. For each material we calculate a self-consistent noninteracting Hamiltonian H^0 through the QSGW formalism. Spin-orbit coupling is neglected, following prior work.^{6,7} Table I shows calculated values at high-symmetry points, compared with available experimental data. As we and others have noted,^{15,16,22} the QSGW gap is systematically overestimated because the RPA underestimates the screening. (Also the GaAs calculation used a smaller basis what was reported in,¹⁵ resulting in an additional overestimate of ~ 0.05 eV.) The QSGW method is one of the most reliable procedure to predict the QP eigenfunctions and eigenvalues, at least as reliable as other methods such as one-shot GW from LDA²³ or exact exchange

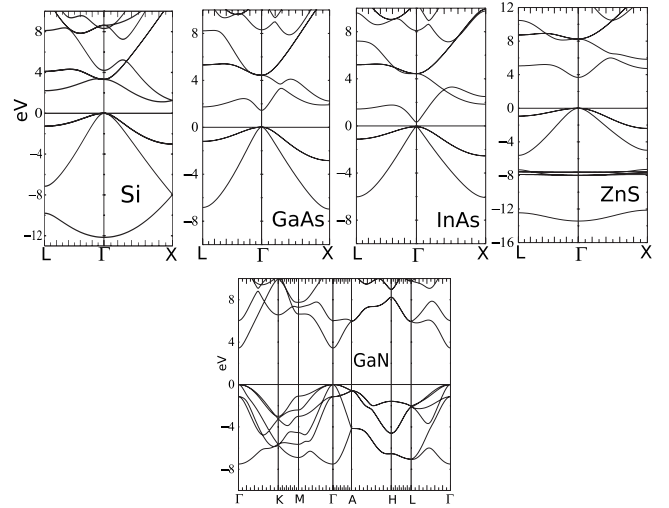


FIG. 1. Energy bands calculated by the QSGW α method [Eq. (9)], with α chosen to reproduce the experimental band gap E_G . In wurtzite GaN, $E_G=3.44$ eV (Ref. 21) and $\alpha=0.79$. Data for other compounds can be found in Table I.

(EXX)-LDA.¹³ To compare the QSGW results to experiment, we must take into account other contributions: spin-orbit coupling, zero-point motion,²⁴ and finite temperature all reduce the gap slightly.²⁵

To obtain the most reliable IIR, we slightly modify H^0 to reproduce the experimental gap at room temperature without including these contributions explicitly. To do this, we add an empirical scaling (“QSGW α ” correction) following the procedure used in Ref. 19. This kind of correction is inevitable even if we start from other first-principle methods when we require 0.1 eV level of accuracy for the QP energies. We scale the one-body Hamiltonian as follows:

$$H^\alpha = H^0 + (1 - \alpha)(\tilde{\Sigma} - V_{xc}^{LDA}), \quad (9)$$

where $\tilde{\Sigma}$ is the static version of the self-energy [see Eq. (10) in Ref. 16]. Table I shows numerical values both with and without the scaling. As we showed in Ref. 19, effective masses are also well reproduced. Thus, we can set up a satisfactory H^α with a single parameter α . This procedure is reasonable because the uncorrected gaps are already close to experiment and $1 - \alpha$ is not large. The materials dependence of α shown in Table I originates largely from the dependence of SO coupling and finite temperature on material. If these were taken into account by improving H^0 explicitly, a universal choice of $\alpha \sim 0.8$ would reproduce the experimental gaps in the Table to within ~ 0.1 eV. (Alternatively, adopting the present procedure with a universal $\alpha \sim 0.75$ accomplishes much the same thing.) Table I shows that the experimental energy dispersions are also well reproduced where they are well known (Si and GaAs). This systematic tendency is found for many other materials, including ZnO, Cu₂O, NiO and MnO,^{14,16} and GdN.¹⁸ It implies that the QSGW α procedure is broadly applicable with comparable accuracy to many environments, e.g., to InAs/GaAs grain boundaries. The QSGW α energy bands are shown in Fig. 1.

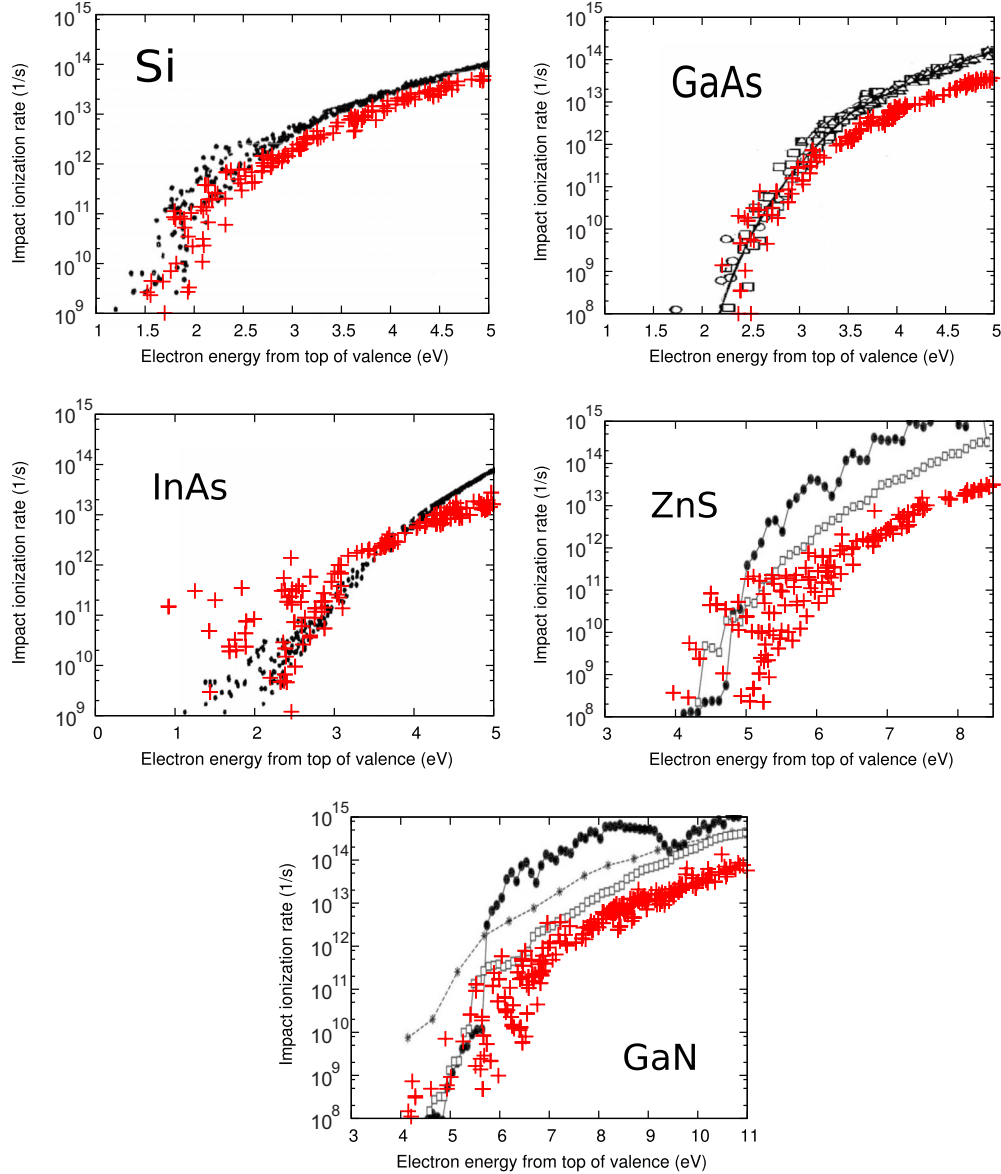


FIG. 2. (Color online) Impact ionization rates τ_{kn}^{-1} as a function of the initial electron energy ε_{in} (measured from the bottom of conduction band). The present GWA calculation is shown by large (red) plus signs. It is superposed on previous calculations: Si and InAs from Sano and Yoshii (Ref. 6), GaAs from Jung *et al.* (Ref. 7), ZnS and GaN from Kuligk *et al.* (Ref. 13). Open boxes in the ZnS and GaN data are screened exchange results from Picozzi *et al.* (Ref. 10); solid circles are exact exchange results (Ref. 13). We used 500 \mathbf{k} points in the 1st Brillouin zone for GaN, and 1728 points for the cubic compounds [regular mesh including the Γ point (Ref. 16)].

Given H^α , we perform a one-shot GWA calculation using the method detailed in Ref. 16, and calculate τ_{kn}^{-1} from Eq. (1). To reduce the computational time we truncate the product basis for each atomic site to $l \leq 1$. This limits the degrees of freedom for the local-field correction in the dielectric function. However, we checked that this little affects the results. To obtain Z_{kn} in Eq. (1), we need to calculate the derivative of the self-energy $\frac{\partial \text{Re} \Sigma(\omega)}{\partial \omega}$ at ε_{kn} , though Z contributes a relatively unimportant factor ~ 0.8 . The main computational cost of the IIR calculation comes from the sum of the pole weights on the real axis; see Eq. (58) in Ref. 16. This corresponds to the convolution of $\text{Im} G$ and $\text{Im} W$, Eq. (2), after $\text{Im} W$ is obtained from integration by the tetrahedron method.¹⁶ This allows us to calculate accurate dielectric

functions with less number of \mathbf{k} points in comparison with simple sampling methods.

Figure 2 shows our results for τ_{kn}^{-1} . The x axis denotes the initial electron energy ε_{in} measured from the bottom of the conduction band; $\varepsilon_{in} > E_G$ is a hard threshold below which IIR is zero. The present results, depicted by large plus signs, are superposed on results taken from previous works. For these calculations, we used 500 \mathbf{k} points in the 1st Brillouin zone for GaN, and $12 \times 12 \times 12 = 1728$ \mathbf{k} points for others with cubic structures (regular mesh including the Γ point¹⁶). Owing to the limited number of \mathbf{k} points, there are some numerical errors; based on our convergence tests by comparing these results with calculations with less number of \mathbf{k} points, we estimate that errors can be a factor of two or so for

the IIR when they are less than $\sim 10^{10} \text{ s}^{-1}$ (the IIR are converged better for the larger IIR). Such errors may sound too large, however, it is not so serious when it is plotted on Fig. 2; note the log scale in y axis. Furthermore, note that the low IIR at low ε_{in} are very sensitive to changes of ε_{in} . Changes of ε_{in} by $\sim 0.1 \text{ eV}$ can easily change the IIR so much, though $\sim 0.1 \text{ eV}$ accuracy of the QP energies is more or less what we expect in our QSGW methods. Thus we think it is not so meaningful to persuade further convergence. In either way, these errors are not large enough to affect our conclusions shown in this paper.

The IIR has a typical feature as already shown in Fig. 1 in Ref. 5, that is, the IIR as function of ε_{in} are widely scattered at low ε_{in} because of the limited number of transitions that conserve energy and momentum. The scatter diminishes at high energy because of an averaging effect which smears the anisotropy in the Brillouin zone as discussed in.⁵ Our results for Si and GaAs correspond rather well to previous works. Details for the IIR are already well analyzed.^{4-7,9,10,13}

Turning to ZnS and GaN, we superpose our results on those presented by Kuligk *et al.* in Figs. 9 and 10 of Ref. 13, which include EXX (solid symbols) and screened exchange results from Ref. 10 (open symbols). The EPP and the present calculations appear mostly similar apart from an approximately constant factor; however the EXX results show rather different behavior, particularly in GaN. This is likely because the EPP and QSGW energy bands are quite similar to each other, but they are quite different from the EXX case (see Figs. 2 and 3 in Ref. 13).

A large discrepancy with EPP is seen only in InAs. Our data is superposed on the calculations by Sano and Yoshii.⁶ We obtain high IIR at low-initial electron energies $\varepsilon_{\text{in}} \geq 1 \text{ eV}$. Such high IIR comes from initial electrons near the conduction band minimum at the Γ point. Since the band gap and effective mass are small in InAs, there are states not far from Γ with energy $\varepsilon_{\text{in}} > E_G$, which can generate an electron-hole pair. This occurs only for InAs in the cases studied, but generally occurs for narrow gap semiconductors. For the discrepancy with results of Sano and Yoshii may be due to their constant matrix elements approximation, which is not suitable for such a narrow gap material [see Ref. 6 near Eq. (2)].

In conclusion, we have calculated the IIR for several materials in the GWA, after a theoretical discussion of its application to the IIR. In principle, the method presented here will be applicable even to inhomogeneous systems such grain boundaries and quantum dots where we expect very strong IIR. The present calculations correspond reasonably well to prior work, with the exception of the narrow gap material InAs. High IIR would be expected universally in similar narrow gap materials such as GaSb, InSb, and InN. This indicates that careful consideration for the IIR might be required when we use such materials for devices.

ACKNOWLEDGMENTS

This work was supported by ONR Contract No. N00014-7-1-0479, and the NSF (Grant No. QMHP-0802216). We are also indebted to the Ira A. Fulton High Performance Computing Initiative.

¹D. K. Ferry, *Semiconductor Transport* (Taylor & Francis, London, 2000).

²R. D. Schaller and V. I. Klimov, *Phys. Rev. Lett.* **92**, 186601 (2004).

³E. O. Kane, *Phys. Rev.* **159**, 624 (1967).

⁴N. Sano and A. Yoshii, *Phys. Rev. B* **45**, 4171 (1992).

⁵N. Sano and A. Yoshii, *J. Appl. Phys.* **75**, 5102 (1994).

⁶N. Sano and A. Yoshii, *J. Appl. Phys.* **77**, 2020 (1995).

⁷H. K. Jung, K. Taniguchi, and C. Hamaguchi, *J. Appl. Phys.* **79**, 2473 (1996).

⁸A. Seidl, A. Görling, P. Vogl, J. A. Majewski, and M. Levy, *Phys. Rev. B* **53**, 3764 (1996).

⁹S. Picozzi, R. Asahi, C. B. Geller, A. Continenza, and A. J. Freeman, *Phys. Rev. B* **65**, 113206 (2002).

¹⁰S. Picozzi, R. Asahi, C. B. Geller, and A. J. Freeman, *Phys. Rev. Lett.* **89**, 197601 (2002).

¹¹T. Kotani, *Phys. Rev. B* **50**, 14816 (1994); **51**, 13903 (1995).

¹²M. Städele, J. A. Majewski, P. Vogl, and A. Görling, *Phys. Rev. Lett.* **79**, 2089 (1997).

¹³A. Kuligk, N. Fitzer, and R. Redmer, *Phys. Rev. B* **71**, 085201 (2005).

¹⁴S. V. Faleev, M. van Schilfgaarde, and T. Kotani, *Phys. Rev.*

Lett. **93**, 126406 (2004).

¹⁵M. van Schilfgaarde, T. Kotani, and S. Faleev, *Phys. Rev. Lett.* **96**, 226402 (2006).

¹⁶T. Kotani, M. van Schilfgaarde, and S. V. Faleev, *Phys. Rev. B* **76**, 165106 (2007).

¹⁷T. Kotani, M. van Schilfgaarde, S. V. Faleev, and A. Chantis, *J. Phys. Condens. Matter* **19**, 365236 (2007).

¹⁸A. N. Chantis, M. van Schilfgaarde, and T. Kotani, *Phys. Rev. B* **76**, 165126 (2007).

¹⁹A. N. Chantis, M. van Schilfgaarde, and T. Kotani, *Phys. Rev. Lett.* **96**, 086405 (2006).

²⁰P. Echenique, J. Pitarke, E. Chulkov, and A. Rubio, *Chem. Phys.* **251**, 1 (2000).

²¹O. Madelung, *Semiconductors—Basic Data*, 2nd ed. (Springer, New York, 1996).

²²M. Shishkin, M. Marsman, and G. Kresse, *Phys. Rev. Lett.* **99**, 246403 (2007).

²³H. Chacham and S. G. Louie, *Phys. Rev. Lett.* **66**, 64 (1991).

²⁴M. Cardona and M. L. W. Thewalt, *Rev. Mod. Phys.* **77**, 1173 (2005).

²⁵M. van Schilfgaarde, T. Kotani, and S. V. Faleev, *Phys. Rev. B* **74**, 245125 (2006).